Tellus (1988), *40A*, 151–161

Observations and model calculations of aerodynamic drag on sea ice in the Fram Strait

By INGER HANSSEN-BAUER and YNGVAR T. GJESSING, *Section of Meteorology, Department of Geophysics, University of Bergen, N-5007 Bergen, Norway*

(Manuscript received January 12; in final form April 1, 1987)

ABSTRACT

Wind and temperature profiles in the constant flux layer obtained by tethersonde were used to compute the total aerodynamic drag on an area of 60% pack ice in the Fram Strait (79°20′N, 1–3°W). The boundary layer appeared adiabatic to heights greater than 150 m, and there were only minor air/water temperature differences. Drag coefficients of 4.9 and $5.1 \cdot 10^{-3}$ referred to 10 m above ground level were found. Eddy correlation measurements in the local constant flux layers over ice floes were used to estimate the skin drag of an area of 100% ice cover. This was less than 40% of the total drag on the actual area. The corresponding drag coefficient was $1.4 \cdot 10^{-3}$. A drag partition model is proposed for computing the total drag over an area of pack ice as a function of ice concentration, mean freeboard and length of the ice floes, and typical roughness lengths of ice and sea surfaces. The model predicts maximum form drag at 73% ice concentration for floes of the type observed in the Fram Strait.

1. Introduction

The location and concentration of pack ice in polar regions greatly influences the exchange of energy between the ocean and atmosphere, and has recently become an important element in the planning of off-shore oil drilling activity in the arctic. The exterior forces affecting an area of pack ice are drags from ocean currents and wind. The drag effect of wind and ice is dependent upon wind speed and ice roughness, and may be expressed as:

$$\tau_t = \rho u_*^2 = \rho C_d(z)\, U^2(z), \tag{1}$$

where ρ is air density, u_* is the friction velocity over an area of drifting ice, $U(z)$ the wind speed at height z above ground level, and $C_d(z)$ the drag coefficient referenced to the same height. U may be determined empirically, and τ_t may then be calculated if C_d is known. Over a horizontal homogeneous area and under steady state conditions, C_d may be determined from measurements obtained from the turbulent surface layer of the turbulent wind components (eddy correlation method) or from wind and temperature profiles (flux-profile method). Since the 1960s, numerous calculations of C_d have been made over different types of pack ice and under different atmospheric conditions (see review in Overland, (1985)). The earliest calculations were based on measurements made in the lowest 4 m of the atmosphere. These measurements can only be used to calculate C_d over areas lacking larger leads (i.e., open lanes in the pack ice) and pressure ridges. Arya (1973, 1975) suggested that Schlichtings (1936) drag partition theory be used to express the total wind drag τ_t over ridged areas as the sum of a skin drag S_d and a form drag F_d:

$$\tau_t = S_d + F_d. \tag{2}$$

S_d is calculated from measurements made at low levels and at distances far from ridges, and F_d from measurements of average height and frequency of ridges in the region. A large-scale drag coefficient can then be calculated from τ_t using eq. (1). Arya concluded that ridges of the heights and frequencies found in Arctic regions could not be neglected when calculating large-scale drag

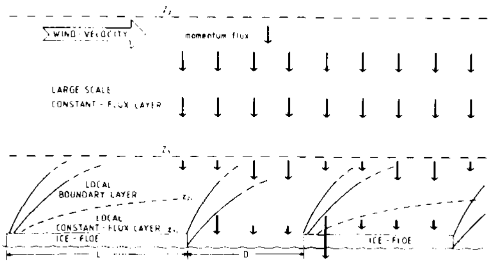

Fig. 1. Sketch of the atmospheric boundary layer over an area of pack ice. Z_1 and Z_2 are the lower and upper boundaries of the large scale constant-flux layer, where the wind speed under adiabatic conditions is given by equation (3) inserted U_* and Z_0. z_{1i} and z_{2i} are the lower and upper boundaries of the local scale constant-flux layer over an ice floe, where the wind speed under adiabatic conditions is given by equation (3) inserted u_{*i} and z_{0i}. L, H and D denote length and freeboard of ice floes, and the distance between floes.

coefficients. More recently it has been common to calculate the total stress directly from measurements of momentum flux and wind speed from an aircraft flying in low height. Mean values are calculated for large areas, thus eliminating the demand for small scale horizontal homogeneity. Consequently, measurements made from airplanes have provided the basis for calculating the large-scale drag coefficient C_d over areas of any ice concentration. It is also possible however, to arrive at the total aerodynamic drag over areas with pressure ridges and leads based on measurements made at one location. This may be accomplished by averaging over wind directions with different upwind roughnesses, or by measuring at such great heights that the horizontal inhomogeneities are smoothed out (Fig. 1).

Measurements from an area in the Fram Strait (79°20′N, 1–3°W) with an ice concentration (i.e., % of the water surface covered by ice) of 60% are presented here. The total drag was calculated from wind and temperature profiles measured in the boundary layer. The local skin drag over the ice surface was calculated from eddy correlations based on measurements made with an acoustic anemometer at a height of 1.7 m. A method is suggested for calculating the total aerodynamic drag over an area in the marginal ice zone under neutral stability, analogous with Arya's (1975) model. Finally, the model is tested with data from the Fram Strait.

2. Theoretical background

Calculations of C_d using the turbulent surface layer temperature and wind profile are based on Monin–Obukhov's (1954) similarity theory which assumes stationarity and horizontal homogeneity. At neutral stability this coincides with Prandtl's (1934) dimensional analysis of the neutral boundary layer which leads to the logarithmic wind profile:

$$U(z) = (u_*/k)\ln(z/z_0). \tag{3}$$

Here k is von Karman's constant, and z_0 is the roughness length. Then at neutral conditions:

$$C_d(z) = \{k/\ln(z/z_0)\}^2. \tag{4}$$

Calculating C_d from measurements of the turbulent wind components is based on the equation:

$$u_*^2 = \langle -u'(z)\,w'(z)\rangle, \tag{5}$$

where $u'(z)$ and $w'(z)$ are the turbulent wind velocities in the main wind direction and the vertical direction at height z above ground level. Angle brackets denote time average.

Both the above mentioned methods for calculating C_d assume that the measurements used were made in the constant flux layer whose borders are here designated by z_1 and z_2. The upper limit z_2 represents the transition to the Ekman layer under ideal conditions of a stationary boundary layer over an unlimited, horizontal homogeneous area. If however, the wind originates from an area with characteristics differing from those of the underlying area, then the requirement of horizontal homogeneity is not satisfied. Eqs. (3) and (5) are still assumed to apply, though z_2 in this instance represents the transition between air in balance with the underlying surface and air still partly influenced by the neighboring region. The lower limit z_1 for the constant flux layer is dependent upon the distance between the largest roughness elements in the area within which stress is to be measured. Large roughness elements appear as horizontal inhomogeneities if measurements are made at too low a level. Measurements from low levels can, nevertheless, be used to calculate the total drag if they are averaged in the horizontal plane.

Fig. 1 illustrates the atmospheric boundary layer over a typical area of pack ice. By calculating the total drag τ_t or its equivalent large-scale roughness length Z_0 over this area, Z_1 and Z_2 will define the lower and upper limit for a constant flux layer with horizontal scale over the entire area.

All measurements must be made in the local constant flux layer above the ice floe when calculating the skin drag S_d and equivalent local roughness length z_{0i}. The lower boundary z_{1i} may be ignored in this case, and the upper boundary z_{2i} increases with increasing distance from the ice edge. It is assumed that the skin drag coefficient, which may be calculated from measurements in the local constant flux layer over an ice floe, is identical with the large-scale drag coefficient when the contribution from the form drag can be ignored, that is when ice concentration is 100% and the area lacks ridges of any significance.

3. Measurements and results

The measurements were made on 26 and 27 July 1983 on ice floes in the Fram Strait at 79°20′N, 1°30′W and 79°22′N, 3°04′W, respectively. The ice cover in both cases was visually estimated to 60% and mean floe size in the area approximately 20 × 20 m. The mean freeboard calculated from measurements in holes drilled in a number of floes in the area was 0.4 m. Drag measurements were made the first day on a floe measuring 60 × 90 m and the second day on a floe measuring 200 × 300 m. The ice surfaces in the area were covered with slushy snow and were slightly hummocked. The mean wind velocity at 5 m height showed nearly stationary wind conditions both days. Aside from occasional passing cloud banks, the cloud cover was approximately the same during each measuring period.

3.1. Total drag and the large-scale drag coefficient

Temperature and wind profiles were measured with an tethersonde system from Atmospheric Instrumentation Research. Three soundings, each of about 45 min, were made on both days. Calculations of the roughness length based on one sounding only are known to be unreliable (Arya, 1975). Therefore the profile measurements presented here are based on three soundings. The soundings were made at different locations on the floe. Figs. 2 and 3 show the combined plots of (a) potential temperature, (b) wind velocity and (c) wind direction for 26 and 27 July. On each day, there was a neutral boundary layer under a stable layer based at about 225 and 150 m, respectively. The wind both days had a strong southerly component, and the stable layer in each instance presumably marked the transition zone between unaffected marine air and air which was more or less influenced by the characteristics of the underlying pack ice. A certain part of this boundary layer (approximately 10% according to Oke,

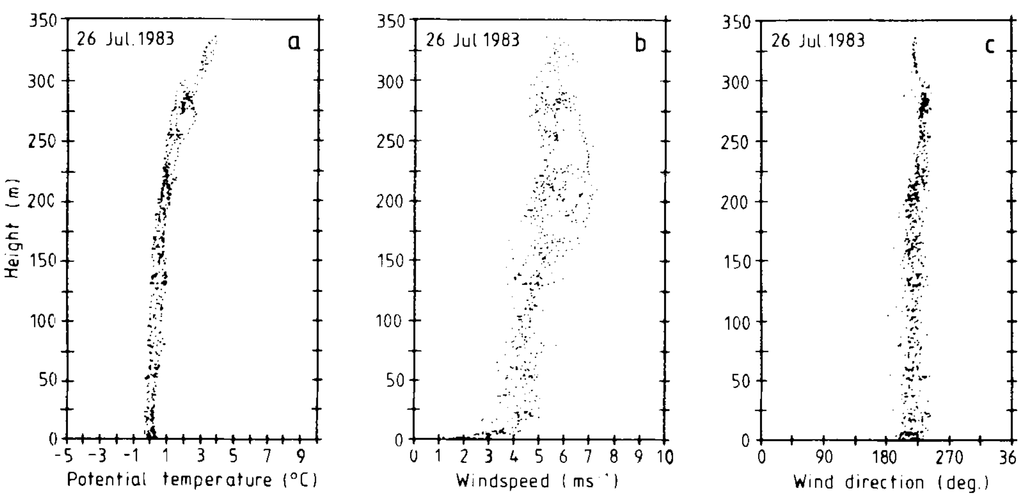

Fig. 2. Vertical profiles of (a) potential temperature (°C), (b) wind speed (ms^{-1}), and (c) wind direction (deg). The profiles were measured on 26 July 1983 10.45–11.30, 12.00–12.50 and 14.10–15.00 GMT.

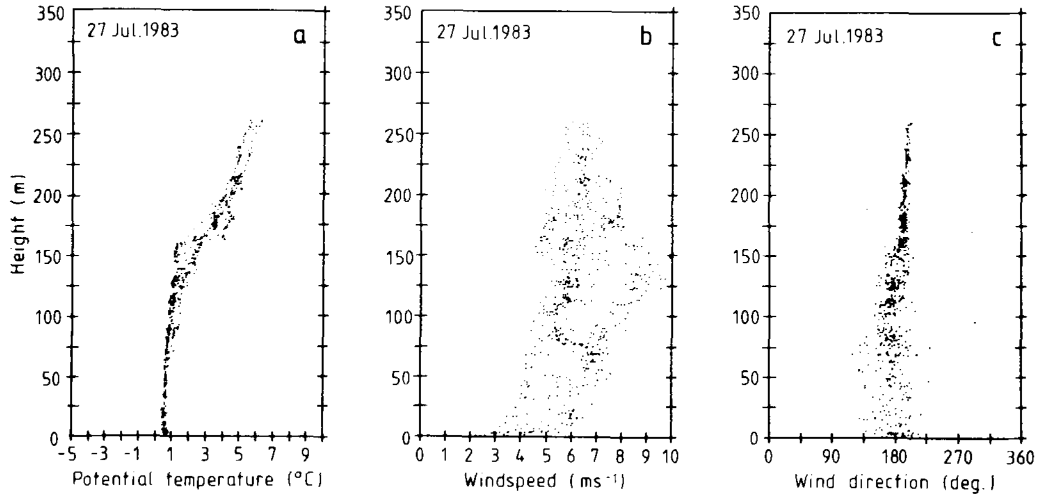

Fig. 3. Vertical profiles of (a) potential temperature (°C), (b) wind speed (ms^{-1}), and (c) wind direction (deg). The profiles were measured on 27 July 1983 14.30–15.15, 15.20–16.00 and 16.05–16.40 GMT.

1978) is fully adjusted to the properties of the new surface.

Table 1 shows the results of the least squares adjustment of all observed values between level z_1 and z_2 to a logarithmic wind profile. The upper boundary Z_2 of the constant flux layer is presumed to be the greatest value z_2 can be assigned, before the calculated values for Z_0 and U_* begin to decline significantly with respect to lower choices of z_2. Consequently, Z_2 is assigned a value of 35 m on 26 July and 20 m on 27 July. Table 1 indicates that when z_1 is assigned a value of 1 m, then Z_0 varies only slightly regardless of whether z_2 is 10 or 20 m. This suggests that deviation from the logarithmic profile due to horizontal inhomogeneity at low levels is less than the deviation found at all levels as a result of fluctuations in wind over time. For this reason, a value of 1 m has been chosen as the lower boundary for the tethersonde measurements that may be used for calculating the large scale Z_0, even if this height is below the large-scale constant flux layer. There are 2 reasons why this low value can be used, despite the obvious presence of horizontal variation at this level. First, the profiles are composed of soundings from different locations on the floe and are therefore to some degree averaged in the horizontal plane. Second, fluctuations within the wind field tend to smooth out horizontal inhomogeneities.

The large-scale roughness length Z_0 was 0.036 and 0.033 m, respectively, over the 2 areas when above values were substituted for Z_1 and Z_2. The corresponding large-scale drag coefficients at 10 m as calculated from eq. (4) are 5.1 and $4.9 \cdot 10^{-3}$. The friction velocity u_* during the time periods involved was 0.261 and 0.345 ms^{-1}, and (τ_t/ρ) was 0.0681 and 0.1190 $m^2 s^{-2}$ as a result.

3.2. *Skin drag over an ice floe and the skin drag coefficient*

Eleven successful 15-min measurement series of the wind components u', v' and w' were conducted on 26 and 27 July at a height of 1.7 m. Measurements were made at different distances from the ice edge to ascertain that the measurements used in the final calculation of S_d were made in the local constant flux layer of the floe. Table 2 shows some of the results of these series. Column 4 shows the friction velocity u_* under conditions of horizontal homogeneity while column 5 shows the skin drag coefficient for an ice surface C_{di} (1.7 m) under such conditions. Horizontal inhomogeneity is thus revealed during instances when the values in column 5 change with changing distance from the edge of the floe. No systematic change was found in these values when the distance to the ice edge was 70 m or more. This indicates that the local constant flux layer over the floe was at least 1.7 m thick when the distance to the ice edge was 70 m. Therefore,

Table 1. *Results of least square adjustment of wind observations between level z_1 and z_2 to the logarithmic wind profile $U = (u_*/k)\, ln(z/z_0)$*

(a) Soundings 26 July 1983 between 10.45 and 15.00 GMT

z_1 (m)	z_2 (m)	n	corr.	p	$u_* \pm$ std. err. (ms^{-1})	z_0 $\langle \pm$ std. err.$\rangle$ (m)
1	10	59	0.79	0.000	0.264 ± 0.027	0.038 ⟨0.026–0.051⟩
1	20	78	0.80	0.000	0.254 ± 0.022	0.033 ⟨0.024–0.043⟩
1	35	100	0.84	0.000	0.261 ± 0.017	0.036 ⟨0.029–0.045⟩
1	50	119	0.82	0.000	0.235 ± 0.015	0.023 ⟨0.018–0.029⟩
5	20	47	0.49	0.001	0.237 ± 0.064	0.021 ⟨0.005–0.048⟩
5	35	69	0.61	0.000	0.255 ± 0.041	0.031 ⟨0.016–0.051⟩
5	50	88	0.54	0.000	0.188 ± 0.032	0.004 ⟨0.001–0.009⟩
10	50	60	0.22	0.010	0.126 ± 0.074	0.000 ⟨0.000–0.002⟩

(b) Soundings 27 July 1983 between 14.30 and 16.45 GMT

z_1 (m)	z_2 (m)	n	corr.	p	$u_* \pm$ std. err. (ms^{-1})	z_0 $\langle \pm$ std. err.$\rangle$ (m)
1	10	38	0.87	0.000	0.343 ± 0.033	0.033 ⟨0.023–0.045⟩
1	20	59	0.84	0.000	0.345 ± 0.030	0.033 ⟨0.024–0.044⟩
1	35	76	0.80	0.000	0.310 ± 0.027	0.021 ⟨0.015–0.029⟩
1	50	102	0.78	0.000	0.295 ± 0.024	0.017 ⟨0.012–0.023⟩
5	20	30	0.36	0.050	0.377 ± 0.184	0.058 ⟨0.004–0.147⟩
5	35	47	0.23	0.126	0.170 ± 0.109	0.000 ⟨0.000–0.004⟩
5	50	73	0.31	0.008	0.200 ± 0.074	0.001 ⟨0.000–0.004⟩
10	50	64	0.15	0.239	0.123 ± 0.104	0.000 ⟨0.000–0.004⟩

The columns of the table give: (1) lower and (2) upper limit for the wind measurements that are used in the least square adjustment to the logarithmic profile, (3) the number of wind observations in the interval, (4) the correlation coefficient between the observations and the profile, (5) the probability value associated with the 2-tailed t-test for regression slopes, (6) the friction velocity and (7) the roughness length for the profile. Values in columns (6) and (7) are shown with ± one standard error.

Table 2. *Results from 15-min measurement series with acoustic anemometer at height 1.7 m and at different distances downwind from ice edge*

Start time	Dist. edge (m)	$\langle U \rangle$ (ms^{-1})	$\sqrt{\langle -u'w' \rangle}$ (ms^{-1})	$\langle -u'w' \rangle / \langle U \rangle^2$
26 July 11.30	15	3.22	0.217	$4.5\ 10^{-3}$
26 July 11.55	15	3.04	0.193	$4.0\ 10^{-3}$
26 July 12.15	15	3.43	0.211	$3.8\ 10^{-3}$
26 July 13.45	70	3.37	0.158	$2.2\ 10^{-3}$
26 July 14.35	70	4.03	0.168	$1.7\ 10^{-3}$
26 July 14.55	90	3.63	0.166	$2.1\ 10^{-3}$
26 July 15.15	90	3.97	0.189	$2.3\ 10^{-3}$
27 July 14.37	70	4.02	0.183	$2.1\ 10^{-3}$
27 July 15.02	70	4.63	0.210	$2.1\ 10^{-3}$
27 July 15.46	180	5.06	0.223	$1.9\ 10^{-3}$
27 July 16.25	180	4.61	0.219	$2.3\ 10^{-3}$
27 July 16.25	180	4.61	0.219	$2.3\ 10^{-3}$

Columns show: (1) starting time for measurement series, (2) distance from measuring place upwind to ice edge, (3) mean horizontal wind, (4) mean local friction velocity, and (5) the relationship between the squares of the friction velocity and the wind velocity (5).

when calculating z_{0i} and u_{*i} for 26 July, only the last 4 measurement series are used. The mean wind speed at 5 m during these periods was 3.79 ms^{-1}, while it was 3.58 ms^{-1} during the sounding periods the same day. All measurement series from 27 July are used and the mean wind was 4.52 ms^{-1}, while it was 4.56 ms^{-1} during the sounding period that day. The final values for z_{0i} calculated from C_{di} (1.7 m) were 0.00025 m on 26 July and 0.00024 m on 27 July. This corresponds to a local scale drag coefficient at 10 m of $1.4 \cdot 10^{-3}$ at neutral stability and over an area where $F_d = 0$. The local friction velocity u_{*i} calculated from the same measurement series was 0.170 and 0.209 ms^{-1} during the same periods. Corresponding values for the sounding periods may be found by correcting for the adjusted mean wind. This gives 0.161 and 0.211 ms^{-1} for 26 and 27 July respectively, and $(S_{di}/\rho) = 0.0259$ and 0.0445 $m^2 s^{-2}$. The total aerodynamic drag over a continuous ice surface would therefore have been less than 40% of the drag over the actual area.

3.3. Comparison with other observations

Over an area of 60% ice cover the drag coefficient was about $5 \cdot 10^{-3}$, which is probably the highest value ever found over pack ice. The roughness of the ice surfaces corresponded to a drag coefficient C_{di} (10 m) of $1.4 \cdot 10^{-3}$, a value which approximates that found for large, comparatively flat floes (Untersteiner and Badgley, 1965; Smith, 1972; Banke et al., 1976). Thus a large part of the contribution to the total drag must come from the edges of individual floes (form drag). Several authors have calculated C_d (10 m) of approximately $3.0 \cdot 10^{-3}$ over areas with about 90% ice concentration (Pease et al., 1983; Walter et al., 1984; Overland, 1985), though few calculations have been made at lower concentrations. Andreas et al. (1984) estimated the drag coefficient at 30% ice concentration to be $2.9 \cdot 10^{-3}$ and at 80% concentration $4.0 \cdot 10^{-3}$ in the Antarctic marginal ice zone. They suggested expressing the drag coefficient as a function of the drag coefficient over open water and the ice concentration, and that this function must have a maximum value for a specific concentration. The ice concentration giving maximum aerodynamic drag however must also be dependent upon both ice thickness and distance between ice floes, since both characteristics influence resistance to wind. The following is a model for calculating the drag coefficient over an area of pack ice under neutral stability. It incorporates the above mentioned parameters and is tested on data from the Fram Strait.

4. Model for calculating the large-scale drag

The total aerodynamic drag over an area of pack ice can be expressed by eq. (2), where S_d represents the skin drag averaged over surfaces of ice and water and F_d the drag caused by the edges of individual floes. A 2-dimensional model for τ_t is developed here. F_d and S_d are parameterized with the help of the ice floe freeboard H, relative length β and ice concentration J. Relative length is defined as $\beta = L/H$, where L is floe length, and ice concentration may be expressed as $J = L/(L+D)$, where D is the distance between ice floes. L, D and H are shown in Fig. 1. According to Arya (1975), laboratory observations indicate that if the sail area per unit surface area is greater than a certain value, the model will give maximum drag. In the present model the total sail area should be replaced by an "effective sail area", as only a proportion of the floe edge functions as a sail if the distance between individual floes is minimal. Use of the model then demands that $[H_{eff}/(L+D)]$ is below a certain limit. This limit is dependent on the type of roughness, and 0.01 is certainly a restrictive value which should be considered as a minimum for the limit rather than an absolute limit for the model's validity.

4.1. Form drag

If P_d is the force per sail area of the roughness elements then:

$$F_d = P_d H/(L+D) = P_d J/\beta. \tag{6}$$

The assumption is that the wind pressure on the floe edge at the windward side, and the drag at the leeward side, is proportional to the square of the wind velocity at the same level. Accordingly, the following equation is valid:

$$P_d = [\alpha\rho/H] \int_0^H U(z)^2 \, dz. \tag{7}$$

The coefficient α is a measure of how much momentum is transferred to the ice floe. α is assumed to be constant for similarly shaped floes with an identical value of β, because the same amount of the wind is believed to bend both above and to the side of such floes. When floes are infinitely far apart such that they no longer influence the wind profile they are subjected to, the wind is given as $U_0(z) = u_{*w}/k \ln(z/z_{0w})$. Force per sail area can then be expressed as:

$$P_{d0} = [\alpha\rho/H] \int_{z_{0w}}^{H} \{[u_{*w}/k] \ln(z/z_{0w})\}^2 \, dz. \tag{8}$$

This gives:

$$P_{d0} = \alpha\rho[u_{*w}/k]^2 \{[\ln(H/(z_{0w} e))]^2 + 1 - 2z_{0w}/H\}. \tag{9}$$

The last two terms on the right hand side of this equation can be dropped when $H \gg z_{0w}$ such that:

$$P_{d0} = \alpha\rho\{U_0(H/e)\}^2, \tag{10}$$

where $U_0(H/e) = u_{*w}/k \ln(H/(z_{0w} e))$. If the floes are close together they will themselves influence the wind profile and it will no longer be logarithmic. Nägeli (1946) measured wind velocity at different distances downwind from shelterbelts of different densities. His results using shelterbelts of high density show that at distance X downwind from a shelterbelt of height Y, the wind speed may be reasonably well approximated by the equation:

$$U = U_0\{1 - \exp(-0.18X/Y)\}, \tag{11}$$

where U_0 is the undisturbed wind speed. Assuming that (11) adequately describes the wind field in the space between floes, then the wind speed for $z < H$ on the windward side of the floe is described by eq. (11), and substituting $X = D$ and $Y = H$. P_d may then be found by substituting U_0 in (10) by U given in (11):

$$P_d = \alpha\rho\{U_0(H/e)\,[1 - \exp(-0.18\beta(1-J)/J)]\}^2. \tag{12}$$

The reduction in form drag has now been regarded as a result of the reduced wind pressure on the ice edge. Alternatively, it may be regarded as the result of a reduction in the effective sail area. This is reduced as H_{eff}/H where H_{eff} is given by:

$$F_d = P_{d0} H_{eff}/(L + D). \tag{13}$$

H_{eff}, with the help of (6) and (12) may be expressed as:

$$H_{eff} = H[1 - \exp(-0.18\beta(1-J)/J)]^2. \tag{14}$$

This function should be used in any definition of the model's area of validity.

In order to find an estimate for α, the definition of "the roughness element drag coefficient in unobstructed wind profile" used by Marshall (1971) is introduced here:

$$C_{f0}(z) \overset{\text{def}}{=} 2P_{d0}/[\rho U_0(z)^2]. \tag{15}$$

According to eq. (10), C_{f0} at height ($z = H/e$) must be equal to 2α as well as constant for all equally shaped objects with the same value of β, if the assumptions made here are valid. Marshall (1971), using measurements made in a wind tunnel, arrived at $C_{f0}(z)$ for cylinders where the ratio between diameter d and the height H varied between 0.5 and 5. According to Marshall's results, C_{f0} appears to be approximately independent of d/H for large values of d/H. One may then assume that the results for cylinders with $d/H = 5$ are valid also when $d/H > 5$, and that these results will hold for cylinder-shaped ice floes. Marshall calculated C_{f0} for several values of z/H. It may therefore be derived for $z = H/e$ if the assumption of logarithmic wind profile is made. Based on Marshall's data, $C_{f0}(H/e) = 1$ was computed for cylinders with $d/H = 5$. Considering the floes as cylinders with $d/H > 5$ the estimate for α becomes 0.5, and F_d over an area of pack ice may then be expressed with the help of eqs. (6) and (12):

$$F_d = \{0.5\rho J/\beta\}\{U_0(H/e) \times [1 - \exp(-0.18\beta(1-J)/J)]\}^2. \tag{16}$$

$U_0(H/e)$ is the predicted wind speed at height H/e when J is 0. Reasonable estimates for z_{0w} can be found in the literature. Large and Pond (1981) give C_d (10 m) $= 1.2 \cdot 10^{-3}$ for open water, which corresponds to $z_{0w} = 1.2 \cdot 10^{-4}$ m.

The form drag can now be expressed relative to $S_{dw0} = \rho u_{*w}^2$, the aerodynamic drag over an ocean surface without ice:

$$F_d/S_{dw0} = 0.5J/\beta\{\ln(H/(z_{0w} e)) \times [1 - \exp(-0.18\beta(1-J)/J)]/K\}^2. \tag{17}$$

Fig. 4a shows F_d/S_{dw0} with $H = 0.4$ m and $z_{0w} = 0.00012$ m plotted as a function of J for $\beta =$ 10, 25, 50, 100 and 1000. $H = 0.2$ m would have given about 20% lower values, and $H = 0.6$ m about 11% greater values for F_d/S_{dw0} if the values for J and β were unchanged. (Note that if L and J are constant, a change in H will also imply a change in the value of β, which increases the change in formdrag.) Values of β less than 10 are unrealistic since floes must have a larger length than total thickness to keep from tipping over.

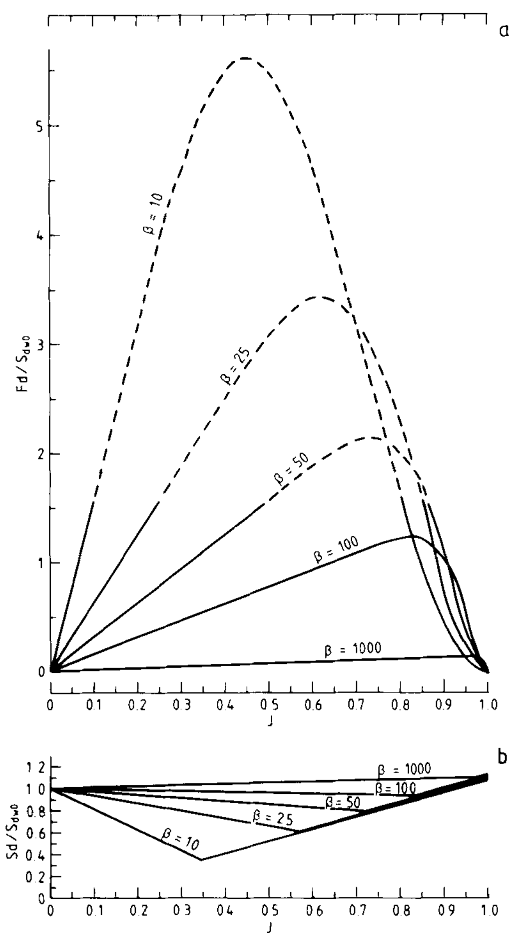

Fig. 4. Drag over an area of pack ice as a function of ice concentration J, shown for different values of the ratio between typical length and height of ice floes β. (a) Form drag when $H = 0.4$ m and $z_{0w} = 0.00012$ m. (b) Skin drag when $z_{0w} = 0.00012$ m and $z_{0i} = 0.00025$ m. Both values are given relative to the skindrag over an area of open water S_{dw0}.

The curves are solid for values corresponding to $H_{eff}/(L + D) < 0.01$.

It is worth mentioning that at very high ice concentrations, the model gives the greatest drag with relatively large ice floes. This is because the distance between small floes at high concentrations is minimal, the result being a small H_{eff}. At low concentrations, H_{eff} approaches H, and many small floes produce greater drag than few large floes.

4.2. Skin drag

The mean skin drag over an area of pack ice can be expressed as:

$$\overline{S_d} = J\overline{S_{di}} + (1 - J)\overline{S_{dw}}. \qquad (18)$$

$\overline{S_{di}}$ and $\overline{S_{dw}}$ are mean values for skin drag over ice and water surfaces respectively. The local values of S_{di} and S_{dw} are assumed to be constant at long distances from the ice edge. However, the wind field will be influenced by the ice edge on the downwind side, and with respect to S_{dw} also on the upwind side. A local intensifying of the wind field may be expected over the floes which leads to an increase in skin drag. Local eddies leading to a decrease in S_{di} may also be expected. The mean value for S_{di} is therefore assumed to approximate the value that S_d would have had over a continuous ice surface, and the following estimate will be applied:

$$\overline{S_{di}} = \rho u_{*i}^2, \qquad (19)$$

where u_{*i} is the friction velocity over an ice surface at such a distance from the ice edge that horizontal homogeneity exists. S_{dw}, as opposed to S_{di}, is always expected to have a lower value near the ice edge than on the open sea, because the wind field is generally weakened both upwind and downwind of floes. The mean skin drag over leads in the pack ice therefore diminishes as leads becomes narrower. This reduction in the mean skin drag, compared to that of an open sea surface, is analogous to the reduction that Arya (1975) modelled into the skin drag for an ice surface with pressure ridges of height H_s within the distance D_s relative to an ice surface without pressure ridges:

$$\overline{S_d(\text{ridged ice})}/\overline{S_d(\text{smooth ice})} = (1 - mH_s/D_s),$$
$$D_s/H_s \gg m. \qquad (20)$$

m is a proportionality factor defined as 20, and Arya uses the equation exclusively when the distance between ridges is large. Here it will also be used for narrow leads such that:

$$\overline{S_{dw}} = (1 - 20H/D)\, S_{dw0} \quad \text{for } D/H > 20, \tag{21a}$$

$$\overline{S_{dw}} = 0 \quad \text{for } D/H \leqslant 20. \tag{21b}$$

The justification for using Arya's equation beyond the area for which it was originally defined is that the skin drag over the water surfaces will comprise an insignificant proportion of the total drag when leads are narrow. Even large relative errors in the estimate of S_{dw} will therefore result in small errors when calculating τ_t and C_d. The mean skin drag over pack ice can then be expressed relative to the total drag over open sea by combining (18), (19) and (21):

$$\overline{S_d}/S_{dw0} = 1 + J\{[u_{*i}/u_{*w}]^2 - 1 - 20/\beta\} \quad \text{for } J < \beta/(20+\beta), \tag{22a}$$

$$\overline{S_d}/S_{dw0} = J[u_{*i}/u_{*w}]^2 \quad \text{for } J \geqslant \beta/(20+\beta). \tag{22b}$$

The wind velocities at the top of the boundary layer Z_2 over an open water surface and an ice covered surface are approximately equal, as the difference in roughness is small. The degree of error is small if we assume:

$$u_{*i} \ln(Z_2/z_{0i}) = u_{*w} \ln(Z_2/z_{0w}). \tag{23}$$

$Z_2 = 20$ m, $z_{0i} = 0.00025$ m and $z_{0w} = 0.00012$ m gives $u_{*i}/u_{*w} = 1.06$. Thus for these values of z_{0i} and z_{0w} the assumption is that (22) may be written:

$$\overline{S_d}/S_{dw0} = 1 + J(0.12 - 20/\beta) \quad \text{for } J < \beta/(20+\beta), \tag{24a}$$

$$\overline{S_d}/S_{dw0} = 1.12J \quad \text{for } J \geqslant \beta/(20+\beta). \tag{24b}$$

These equations are plotted as a function of J for $\beta = 10$, 25, 50, 100 and 1000 in Fig. 4b.

4.3. *Estimating total drag based on data from the Fram Strait*

Table 3 shows the results of the model using the data presented in Section 3. In this instance, u_{*i} is measured and u_{*w} may then be calculated from (23), after which S_d/ρ and F_d/ρ may be derived from (17) and (22a). The sum of these should provide an estimate for U_*^2. In both situations the model gives reasonably good estimates for the drag. There are several possible explanations for why the estimates are slightly lower than the observed values: the effect of form drag on ridges is neglected in the model; the estimate of α could be too low, because cylinders probably give rise to less drag than ice floes; the similarity between wind fields in the vicinity of shelterbelts and ice floes might be slight, as even high density shelterbelts let some wind pass

Table 3. *Observed and modelled aerodynamic drag over an area of pack ice in the Fram Strait 26 and 27 July 1983*

		26 July	27 July
Observations:	J	60%	60%
	L	20 m	20 m
	H	0.4 m	0.4 m
	Z_0	0.036 m	0.033 m
	U_*	0.261 ms^{-1}	0.345 ms^{-1}
	z_{0i}	0.00025 m	0.00025 m
	u_{*i}	0.161 ms^{-1}	0.211 ms^{-1}
Estimates:	z_{0w} (Large & Pond)	0.00012 m	0.00012 m
	u_{*w} (eq. 29)	0.152 ms^{-1}	0.199 ms^{-1}
Observed value:	$\tau_t/\rho = U_*^2$	0.0681 (ms^{-1})^2	0.1190 (ms^{-1})^2
Modelled values:	S_d/ρ	0.0192 (ms^{-1})^2	0.0329 (ms^{-1})^2
	F_d/ρ	0.0436 (ms^{-1})^2	0.0747 (ms^{-1})^2
	$(F_d + S_d)/\rho$	0.0628 (ms^{-1})^2	0.1076 (ms^{-1})^2

through. Besides, the model does not distinguish between different distributions of floe sizes around the mean value L.

5. Summary and conclusions

Calculations of the large-scale drag coefficients based on profile measurements over areas of 60% ice concentration in the Fram Strait resulted in larger values than previously found over pack ice. This is probably caused by a large contribution to the drag from the form drag on ice edges. A model for calculating the total wind drag as a function of ice concentration, freeboard and mean floe size has been developed. A test of the model on data from the Fram Strait resulted in aerodynamic drag less than 10% lower than the observed values.

According to the model, it is the relationship between floe size and free board that determines which ice concentration gives the greatest drag. The model predicts maximum form drag at 73% concentration for floes of the type observed in the Fram Strait. The fact that none of the earlier drag observations were made at medium ice concentrations may explain why the drag coefficient found in this investigation is higher than those found earlier.

The model can be expected to overestimate the drag for small values of β and medium ice concentrations (Fig. 4a), as stagnant flow patterns over and between floes may develop, thereby reducing the total drag. This makes the model unsuitable for predicting the maximum drag coefficient that may be expected over pack ice. A detailed evaluation of the model would require more field data. Qualitatively however the model indicates that even larger drag coefficients may be found over pack ice than those found here.

6. Acknowledgements

The authors are indebted to Assistant Professor Ivar Dugstad and Professor Hans Økland for critical remarks, to Frank Cleveland for drawing the figures, and to Howard Parker for translating the manuscript into English.

7. Appendix. List of symbols

$C_d(z)$	drag coefficient referenced to height z above ground level	dimensionless
$C_{di}(z)$	drag coefficient over 100% ice cover	dimensionless
$C_{dw}(z)$	drag coefficient over sea surface	dimensionless
$C_{r0}(z)$	unobstructed roughness element drag coefficient	dimensionless
D	typical distance between ice floes	m
D_s	mean distance between pressure ridges	m
d	diameter of cylinder	m
F_d	form drag	N m^{-2}
H	typical freeboard of ice floes	m
H_s	mean pressure ridge height	m
H_{eff}	effective freeboard of ice floes	m
J	ice cover $\in [0, 1]$	dimensionless
$K = 0.4$	von Karman's constant	dimensionless
L	typical length of ice floes	m
m	proportionality factor	dimensionless
n	sample size	
p	probability associated with 2-tailed t-test	
P_d	force per frontal area of roughness elements	N m^{-2}
P_{d0}	force per frontal area of roughness elements in unobstructed wind profile	N m^{-2}
S_d	skin drag	m^{-2}
S_{di}	skin drag on an ice surface	m^{-2}

S_{dw}	skin drag on a sea surface	N m^{-2}
$S_{dw0} = \rho u_{*w}^2$	skin drag on a sea surface at long distance from ice floes	N m^{-2}
$U(z)$	wind speed at height z above ground level	ms^{-1}
$U_0(z)$	unobstructed wind profile	ms^{-1}
U_*	friction velocity over an area of drifting ice	ms^{-1}
u_{*0}	friction velocity	ms^{-1}
u_{*i}	friction velocity over an ice surface	ms^{-1}
u_{*w}	friction velocity over a sea surface	ms^{-1}
u', v', w'	turbulent velocities in wind direction, normal to the wind direction, and vertical	ms^{-1}
X	distance upwind to an object	m
Y	height of object	m
Z_0	large-scale roughness length	m
Z_1, Z_2	lower/higher limit of large-scale constant flux layer	m
z_0	roughness length	m
z_1, z_2	lower/higher limit of constant flux layer	m
z_{0i}	roughness length for ice surface	m
z_{1i}, z_{2i}	lower/higher limit of local constant flux layer over ice floes	m
z_{0w}	roughness length for sea surface	m
α	proportionality factor	dimensionless
$\beta = L/H$	relative length of ice floes	dimensionless
ρ	air density	kg m^{-3}
$\tau_t = \rho U_*^2$	total aerodynamic drag	N m^{-2}
$\langle\ \rangle$	time mean	
—	space mean	

REFERENCES

Andreas, E. L., Tucker III, W. B. and Ackley, S. F. 1984. Atmospheric boundary-layer modifications, drag coefficient, and surface heat flux in the Antarctic marginal ice zone. *J. Geophys. Res. 89*, 649–661.

Arya, S. P. S. 1973. Contribution of form drag on pressure ridges to the air stress on Arctic ice. *J. Geophys. Res. 78*, 7092–7099.

Arya, S. P. S. 1975. A drag partition theory for determining the large-scale roughness parameter and wind stress on the Arctic pack ice. *J. Geophys. Res. 80*, 3447–3454.

Banke, E. G., Smith, S. D. and Anderson, R. J. 1976. Recent measurements of wind stress on Arctic sea ice. *J. Fish. Res. Board. Can. 33*, 2307–2317.

Large, W. G. and Pond, S. 1981. Open ocean momentum flux measurements in moderate to strong winds. *J. Phys. Oceanogr. 11*, 324–336.

Marshall, J. K. 1971. Drag measurements in roughness arrays of varying density and distribution. *Agr. Meteorol. 8*, 269–292.

Monin, A. S. and Obukhov, A. M. 1954. Dimensionless characteristics of turbulence in the surface layer. *Akad. Nank. SSSR, Geofiz Inst., Tr. 24*, 163–187.

Nägeli, W. 1946. Further investigation of the wind conditions in areas with shelterbelts (in German). *Mitt. Schweiz. Anstalt Forstl. 24*, 659–737.

Oke, T. R. 1978. *Boundary layer climates* (ed. T. R. Oke). London: Methuen & Co. Ltd., p. 137.

Overland, J. E. 1985. Atmospheric boundary layer structure and drag coefficients over sea ice. *J. Geophys. Res. 90*, 9029–9049.

Pease, C. H., Salo, S. A. and Overland, J. E. 1983. Drag measurements for first-year sea ice over shallow sea. *J. Geophys. Res. 88*, 2853–2862.

Prandtl, L. 1934. The mechanics of viscous fluids. *Aerodynamic Theory, Vol. 3* (ed. W. F. Durand). Berlin: Springer-Verlag.

Schlichting, H. 1936. Experimental investigation of roughness problems (in German). *Ingr. Arch. 7*, 1–34.

Smith, S. D. 1972. Wind stress and turbulence over a flat ice floe. *J. Geophys. Res. 77*, 3886–3901.

Untersteiner, N. and Badgley, F. I. 1965. The roughness parameters of sea ice. *J. Geophys. Res. 70*, 4573–4577.

Walter, B. A., Overland, J. E. and Gilmer, R. O. 1984. Air–ice drag coefficients for first-year sea ice derived from aircraft measurements. *J. Geophys. Res. 89*, 3550–3560.